Comparison of Objective Stress Rates for Explicit Transient Shell Dynamics Analysis

Jason Har†

쉘 구조물의 과도동적거동해석에 적용된 응력률들의 비교

하재선

Key Words : Constitutive Equation(구성방정식), Obejective stress rate(객관응력률), Transient shell dynamics(과도동적쉘해석), Hypo elasto-plasticity(하이포 탄소성)

Abstract

This paper presents applications of the objective stress rates to stress update algorithms for transient shell dynamic analysis within the context of explicit time integration. The hypo elasto-plastic materials are assumed in establishing constitutive equations. The derivation of the objective stress rates are investigated by use of the Lie derivative. Comparison results are given between the Kirchhoff and Cauchy stress formulation. The Jacobian determination algorithm proposed in this paper is presented in association with the Belytschko-Lin-Tsay shell theory. Several numerical examples are demonstrated including contact and non-contact examples, by which proposed algorithms are compared with respect to the accuracy and effectiveness.

1. Introduction

The key issue in computational plasticity is how to establish and to integrate a constitutive equation as a material undergoes elastic-plastic deformation, when a deformation history is assumed to be given. At this point, it is very importantly noted that the stress should be on the yield surface when the material exhibits plastic deformation. For infinitesimal deformation including small rotations, a constitutive equation for hypo elastic-plastic materials can be in rate form established by the material time derivative of the Cauchy stress tensor and the rate of deformation tensor. However, for the case of finite deformation including large deformations and/or large rotations, stress rates retaining material objectivity or the material frame indifference are employed instead of the material time derivative of the Cauchy stress tensor in the constitutive equations of hypo-elastic materials [1, 2]. As discussed next, the material objectivity of the material time derivative of the Cauchy stress tensor disappears unless the time increment size is very small [3].

As an objective stress rate, the Zarembar-Jaumann-Noll stress rate or shortly, the Jaumann stress rate, had been considered most popular before it was unveiled that the nature of the Jaumann stress rate discloses a spurious oscillation for a hypo-elastic material in simple shear. Dienes [4] suggested the replacement to the Jaumann stress rate should be the Green-McInnis-Naghdi stress rate. Johnson and Bammann [5] showed that the use of the Jaumann stress rate in the generalization of the infinitesimal theory leads to an oscillatory response in the evolution of the yield surface in simple shear, and a monotonic increasing shear stress might be achieved by utilization of the Green-Naghdi stress rate. Hence, most of main large scale simulation hydrocodes, nowadays, took the replacement of the Green-Naghdi stress rate instead of the Jaumann stress rate due to its anomaly [4]. However, the anomaly does not manifest itself at shear strains less than 0.4 [4]. It is noted that the vast majority of solid dynamics problems fall into this category. The most widely used stress rates include the Zarembar-Jaumann-Noll stress rate, the Green-McInnis-Naghdi stress rate, and the Truesdell stress rate [6]. What is more,

† Korea Institute of Aerospace Technology, Korean Air
E-mail : mephdjh@krpost.net
TEL : (042) 868-6272 FAX : (042) 868-6128

lots of stress rates are found in the literature such as the Oldroyd stress rate [7], the Durban-Baruch stress rate, the Cotter-Rivlin stress rate [8], the Szabó-Balla stress rate, the twirl tensor of the Eulerian triad stress rate, the twirl tensor of the Lagrangian triad stress rate, and the logarithmic stress rate.

The present paper presents comparison of transient shell dynamics results obtained by the application of a unified stress update algorithm in association with objective corotational stress rates. The stress update algorithm of the radial return method [9], presented by the author in the conference of Solid and Structural Mechanics Division of KSME 2003, is here, divided into two braches including the Cauchy stress formulation and the Kirchhoff stress formulation. The Cauchy stress formulation means that the objective stress rates are expressed in terms of the Cauchy stress tensor, while the Kirchhoff stress formulation means that the objective stress rates are expressed in terms of the Kirchhoff stress tensor. By use of the Lie derivative based on the push-forward and pull-back concept, a series of objective stress rates has been derived in this paper. The present, then, research covers the Cauchy and Kirchhoff stress formulation of the objective stress rates such as the Jaumann rate, Truesdell rate, Oldroyd rate, Cotter-Rivlin rate, and Green-Naghdi rate to integrate hypo elasto-plastic constitutive equations. An explicit finite element implementation based on the Belytschko-Lin-Tsay shell element generation theory [13] for the transient shell dynamics problems will be conducted.

As a **transient shell dynamics example**, a spherical cap clamped all round and subjected to a uniform pressure is demonstrated. As a **contact-impact problem**, a pipe whip problem is presented, namely, one pipe is contacting another one whose circumferences at both ends are fixed.

2. Preliminaries

Let us consider a solid continuum body occupying an open set $\mathcal{B}$ in the three dimensional Euclidean space, $\mathbb{R}^3$, namely $\mathcal{B} \subset \mathbb{R}^3$. A configuration represents a state of the body. Therefore, the position vector of a continuum particle constituting the undeformed body is denoted by $\boldsymbol{X} = \left(X^1, X^2, X^3 \right) \in \bar{\mathcal{B}} \subset \mathbb{R}^3$. The corresponding covariant basis, then, is denoted as a set $\left\{ \boldsymbol{E}^A | A = 1,2,3 \right\}$, and their covariant base vectors are unit Cartesian vectors. As the body moves, we obtain a series of configurations. If our attention is restricted to an interval of time $\mathcal{T} = [0, T]$, a smooth motion of the body is described as a one-to-one mapping:

$$\varphi(X,t) : \bar{\mathcal{B}} \times \mathcal{T} \to \bar{\mathcal{S}} \subset \mathbb{R}^3, \quad \forall t \in \mathcal{T}, \tag{1}$$

where $\bar{\mathcal{S}}$ denotes a closure of the body in the spatial or current configuration. Hence, we have a new configuration representing a deformed state of the body, which are described by another contravariant set $\mathcal{X} = \left\{ x^a \mid a = 1,2,3 \right\} \in \bar{\mathcal{S}} \subset \mathbb{R}^3$. In the same manner, the position vector of a continuum particle constituting the deformed body is denoted by $\boldsymbol{x} = \left(x^1, x^2, x^3 \right) \in \bar{\mathcal{S}} \subset \mathbb{R}^3$. The covariant basis, then, is denoted as $\left\{ \boldsymbol{e}^a | a = 1,2,3 \right\}$, and their covariant base vectors are also unit Cartesian vectors. The deformation gradient tensor is the material gradient of $\boldsymbol{x}$, as defined in terms of unit Cartesian base vectors as:

$$\boldsymbol{F} = \frac{\partial \boldsymbol{x}}{\partial \boldsymbol{X}} = \frac{\partial x^i}{\partial X^J} \boldsymbol{e}_i \otimes \boldsymbol{E}^J = F^i_{\ J} \boldsymbol{e}_i \otimes \boldsymbol{E}^J . \tag{2}$$

Also the deformation gradient tensor can be expressed in terms of generalized base vectors as:

$$\boldsymbol{F} = \frac{\partial \boldsymbol{x}}{\partial \boldsymbol{X}} = \boldsymbol{g}_i \otimes \boldsymbol{G}^i , \tag{3}$$

Where $\boldsymbol{g}_i$ are the covariant base vectors in the deformed local configuration, while $\boldsymbol{G}^i$ are the contravariant base vectors in the undeformed configuration. By the way, the inversed deformation gradient tensor is the spatial gradient of $\boldsymbol{X}$, as given below:

$$\boldsymbol{F}^{-1} = \frac{\partial \boldsymbol{X}}{\partial \boldsymbol{x}} = \boldsymbol{G}_i \otimes \boldsymbol{g}^i . \tag{4}$$

The contravariant and covariant base vectors have the following relations each other

$$\begin{aligned} &\boldsymbol{g}_i = \boldsymbol{F} \cdot \boldsymbol{G}_i, \ \boldsymbol{g}^i = \boldsymbol{F}^{-1} \cdot \boldsymbol{G}^i , \\ &\boldsymbol{G}_i = \boldsymbol{F}^{-T} \cdot \boldsymbol{g}_i, \ \boldsymbol{G}^i = \boldsymbol{F}^T \cdot \boldsymbol{g}^i \end{aligned} . \tag{5}$$

The Kirchhoff stress tensor $\boldsymbol{\tau}$ is given in terms of a push-forward operation φ_*

$$\boldsymbol{\tau} = \varphi_* \left(\boldsymbol{S} \right) = \boldsymbol{F} \cdot \boldsymbol{S} \cdot \boldsymbol{F}^T = \tau^{ij} \boldsymbol{g}_i \otimes \boldsymbol{g}_j , \tag{6}$$

where $\boldsymbol{S}$ is the second Piolar-Kirchhoff stress tensor. On the contrary, the second Piolar-Kirchhoff stress is expressed as:

$$\boldsymbol{S} = \varphi^* \left(\boldsymbol{\tau} \right) = \boldsymbol{F}^{-1} \cdot \boldsymbol{\tau} \cdot \boldsymbol{F}^{-T} = S^{ij} \boldsymbol{G}_i \otimes \boldsymbol{G}_j . \tag{7}$$

Hence, equation (7) shows a pull-back operation for a second order tensor with contravariant components.

When we consider only the mechanical process in which thermal effects are ignored such as in the isothermal or isentropic and adiabatic processes, the rate of internal energy coincides with the rate of the Helmholtz free energy. For the mechanical process only, the stored energy function or strain energy function w are used. Hence we have

$$\rho_0 \dot{W} = J \boldsymbol{\sigma} : \boldsymbol{d} = \boldsymbol{\tau} : \boldsymbol{d} , \tag{8}$$

where $\dot{W}$ is the rate of the stored energy function in the undeformed configuration, J is the Jacobian between the reference and spatial configurations, and $\boldsymbol{d}$ is the

velocity strain tensor. When pull-back operations are applied to the above equation, we find that

$$\rho_0 \dot{W} = \boldsymbol{S} : \dot{\boldsymbol{E}}, \tag{9}$$

where $\dot{\boldsymbol{E}}$ is the rate of the Green-Lagrangian strain tensor. Green defined an elastic material as one for which a strain energy function exists. Truesdell [12] called the material hyperelastic. From the definition of the second Piolar-Kirchhoff stress tensor, the rate-type equation can be derived as:

$$\dot{\boldsymbol{S}} = \rho_0 \frac{\partial^2 \overline{W}}{\partial \boldsymbol{E} \partial \boldsymbol{E}} : \dot{\boldsymbol{E}} = 4\rho_0 \frac{\partial^2 \widehat{W}}{\partial \boldsymbol{C} \partial \boldsymbol{C}} : \frac{1}{2}\dot{\boldsymbol{C}}, \tag{10}$$

Notice that from equation (10), we have the so-called second elasticity tensor as:

$$\mathbb{C} = \rho_0 \frac{\partial^2 \overline{W}}{\partial \boldsymbol{E} \partial \boldsymbol{E}} = C^{ijkl} \boldsymbol{G}_i \otimes \boldsymbol{G}_j \otimes \boldsymbol{G}_k \otimes \boldsymbol{G}_l \tag{11}$$

It should be noted that the push-forward operation of the left-side term in equation (10) is equivalent to the Lie-derivative of the Kirchhoff stress tensor $L_v(\boldsymbol{\tau})$ as follows:

$$\varphi_* \left(\dot{\boldsymbol{S}} \right) = \varphi_* \left[\frac{D}{Dt} \left\{ \varphi^* (\boldsymbol{\tau}) \right\} \right] = L_v (\boldsymbol{\tau}). \tag{12}$$

Since the push-forward operation of $\dot{\boldsymbol{E}}$ yields in the spatial description,

$$\varphi_* \left(\dot{\boldsymbol{E}} \right) = \boldsymbol{F}^{-T} \cdot \dot{\boldsymbol{E}} \cdot \boldsymbol{F}^{-1} = \boldsymbol{d} = L_v (\boldsymbol{e}), \tag{13}$$

equation (10) results in

$$L_v (\boldsymbol{\tau}) = \varphi_* (\mathbb{C}) : \boldsymbol{d} = \mathbb{c} : \boldsymbol{d} = \mathbb{c} : L_v (\boldsymbol{e}), \tag{14}$$

where $\mathbb{c}$ is called the fourth elasticity tensor or spatial elasticity tensor and it can be expressed as

$$\mathbb{c} = c^{ijkl} \boldsymbol{g}_i \otimes \boldsymbol{g}_j \otimes \boldsymbol{g}_k \otimes \boldsymbol{g}_l. \tag{15}$$

Due to Doyle and Ericksen [10], the spatial elasticity tensor $\mathbb{c}$ is given by

$$\mathbb{c} = 2\frac{\partial \boldsymbol{\tau}}{\partial \boldsymbol{g}} = 4\rho \frac{\partial \overline{\overline{W}}(\boldsymbol{g})}{\partial \boldsymbol{g} \partial \boldsymbol{g}}. \tag{16}$$

Notice that $\varphi_* (\mathbb{C}) = \mathbb{c}$. It, hence, should be noticed that in the convected coordinates the contravariant components between the Lagrangian coordinates and Eulerian coordinates are equivalent each other. If we use the same rectangular Cartesian coordinates for both the undeformed and the deformed configurations of the body such as in the isoparametric finite element formulation, we have

$$\boldsymbol{G}_I = \boldsymbol{E}_I, \quad \boldsymbol{g}_i = \frac{\partial x^j}{\partial X^i} \boldsymbol{e}_j = F^i_{\ .I} \boldsymbol{e}_j. \tag{17}$$

In the end, since $\boldsymbol{E}_i = \boldsymbol{e}_i$, we observe that in the rectangular Cartesian coordinates

$$c^{ijkl} = C^{IJKL} F^i_{\ .I} F^i_{\ .J} F^i_{\ .K} F^i_{\ .L}. \tag{18}$$

$L_v (\boldsymbol{\tau})$ leads to the convected rate or the Oldroyd rate [7] of the Kirchhoff stress as:

$$L_v (\boldsymbol{\tau}) = \boldsymbol{\tau}^{\nabla O} = \dot{\boldsymbol{\tau}} - \boldsymbol{l} \cdot \boldsymbol{\tau} - \boldsymbol{\tau} \cdot \boldsymbol{l}^T, \tag{19}$$

where $\boldsymbol{l}$ is the spatial velocity gradient tensor. $L_v (\boldsymbol{\tau})$ is an objective stress rate for which the contravariant components are consider. For the covariant components of the spatial second-order tensor, the Lie derivative yields the Cotter-Rivlin stress rate as shown below:

$$L_v \left(\boldsymbol{\tau} = \tau_{ij} \boldsymbol{g}^i \otimes \boldsymbol{g}^j \right) = \boldsymbol{\tau}^{\nabla CR} = \dot{\boldsymbol{\tau}} + \boldsymbol{l} \cdot \boldsymbol{\tau} + \boldsymbol{\tau} \cdot \boldsymbol{l}^T. \tag{20}$$

The Oldroyd stress rate of the Kirchhoff stress can be expressed as

$$L_v (\boldsymbol{\tau}) = J \left(\dot{\boldsymbol{\sigma}} - \boldsymbol{l} \cdot \boldsymbol{\sigma} - \boldsymbol{\sigma} \cdot \boldsymbol{l}^T + (\boldsymbol{d} : \boldsymbol{I}) \boldsymbol{\sigma} \right) = J \boldsymbol{\sigma}^{\nabla T}, \tag{21}$$

where $\boldsymbol{\sigma}^{\nabla T}$ is the Truesdell stress rate of the Cauchy stress. For the contra-covariant or covariant-contravariant components, we have

$$\begin{aligned} L_v \left(\tau^i_{\ .j} \boldsymbol{g}_i \otimes \boldsymbol{g}^j \right) &= \boldsymbol{\tau}^{\nabla m1} = \dot{\boldsymbol{\tau}} - \boldsymbol{l} \cdot \boldsymbol{\tau} + \boldsymbol{\tau} \cdot \boldsymbol{l}, \\ L_v \left(\tau^{\ j}_{i.} \boldsymbol{g}^i \otimes \boldsymbol{g}_j \right) &= \boldsymbol{\tau}^{\nabla m2} = \dot{\boldsymbol{\tau}} + \boldsymbol{l}^T \cdot \boldsymbol{\tau} - \boldsymbol{\tau} \cdot \boldsymbol{l}^T \end{aligned}, \tag{22}$$

From equation (22), the Jaumann stress rate of the Kirchhoff stress can be derived as

$$\boldsymbol{\tau}^{\nabla J} = \frac{1}{2} \left(\boldsymbol{\tau}^{\nabla m1} + \boldsymbol{\tau}^{\nabla m2} \right) = \dot{\boldsymbol{\tau}} + \boldsymbol{\tau} \cdot \boldsymbol{w} - \boldsymbol{w} \cdot \boldsymbol{\tau}. \tag{23}$$

where $\boldsymbol{w}$ is the spin tensor. It is noted that the Jaumann stress rate of the Cauchy stress may be written as:

$$\boldsymbol{\sigma}^{\nabla J} = \dot{\boldsymbol{\sigma}} + \boldsymbol{\sigma} \cdot \boldsymbol{w} - \boldsymbol{w} \cdot \boldsymbol{\sigma}. \tag{24}$$

The polar decomposition states that any deformation gradient tensor can be multiplicatively decomposed into the product of the rotation tensor $\boldsymbol{R}$ and the right stretch tensor $\boldsymbol{U}$ or the left stretch tensor as shown below:

$$\boldsymbol{F} = \boldsymbol{R} \cdot \boldsymbol{U} = \boldsymbol{V} \cdot \boldsymbol{R}. \tag{25}$$

Introducing the intermediate base vectors $\tilde{\boldsymbol{G}}$ and $\tilde{\boldsymbol{g}}$, we observe that

$$\tilde{\boldsymbol{g}}_i = \boldsymbol{U} \cdot \boldsymbol{G}_i, \boldsymbol{U} = \tilde{\boldsymbol{g}}_i \otimes \boldsymbol{G}^i, \boldsymbol{g}_i = \boldsymbol{R} \cdot \tilde{\boldsymbol{g}}_i, \ \boldsymbol{R} = \boldsymbol{g}_i \otimes \tilde{\boldsymbol{g}}^i, \tag{26}$$

$$\tilde{\boldsymbol{G}}_i = \boldsymbol{R} \cdot \boldsymbol{G}_i, \ \boldsymbol{R} = \tilde{\boldsymbol{G}}_i \otimes \boldsymbol{G}^i, \boldsymbol{g}_i = \boldsymbol{V} \cdot \tilde{\boldsymbol{G}}_i, \ \boldsymbol{V} = \boldsymbol{g}_i \otimes \tilde{\boldsymbol{G}}^i, \tag{27}$$

The push-back operation of the spatial identity tensor under the rotation part $\boldsymbol{R}$ of $\boldsymbol{F}$ becomes

$$\boldsymbol{R}^* \left(\boldsymbol{g} = \boldsymbol{g}_i \otimes \boldsymbol{g}^i = g_{ij} \boldsymbol{g}^i \otimes \boldsymbol{g}^j \right) = \boldsymbol{R}^T \cdot \boldsymbol{g} \cdot \boldsymbol{R}. \tag{28}$$

From equation (26), we have

$$\boldsymbol{R}^{-1} = \tilde{\boldsymbol{g}}_i \otimes \boldsymbol{g}^i, \ \boldsymbol{R}^T = \tilde{\boldsymbol{g}}^i \otimes \boldsymbol{g}_i. \tag{29}$$

Hence, we have

$$\boldsymbol{R}^* (\boldsymbol{g}) = \tilde{\boldsymbol{g}}_i \otimes \boldsymbol{g}^i \cdot \boldsymbol{g}_j \otimes \boldsymbol{g}^j \cdot \boldsymbol{g}_k \otimes \tilde{\boldsymbol{g}}^k = \tilde{\boldsymbol{g}}_i \otimes \tilde{\boldsymbol{g}}^i = \boldsymbol{I} = \tilde{\boldsymbol{g}}. \tag{30}$$

It should be noted that equation (30) is not equivalent to the same expression as in [11; 204]. Furthermore, the push-back operation of $\tilde{\boldsymbol{g}}$ under the rotation part $\boldsymbol{U}$ of $\boldsymbol{F}$ shows that

$$\boldsymbol{U}^* \left(\tilde{\boldsymbol{g}} = \tilde{\boldsymbol{g}}_i \otimes \tilde{\boldsymbol{g}}^i \right) = \boldsymbol{U}^T \cdot \tilde{\boldsymbol{g}} \cdot \boldsymbol{U}. \tag{31}$$

From equation (26), we have

$$\boldsymbol{U}^T = \boldsymbol{G}^i \otimes \tilde{\boldsymbol{g}}_i. \tag{32}$$

Hence, we find that

$$\boldsymbol{U}^* \left(\tilde{\boldsymbol{g}} \right) = \boldsymbol{C}, \tag{33}$$

where $\boldsymbol{C}$ is the right Cauchy Green strain tensor.

Provided that $\tilde{\boldsymbol{g}}$ is referred to as an intermediate configuration being usually called the unrotated configuration, the unrotated stress tensor $\tilde{\boldsymbol{\tau}}$ of the Kirchhoff stress can be written as

$$\tilde{\boldsymbol{\tau}} = \boldsymbol{R}^{*}\left(\boldsymbol{\tau}\right) = \boldsymbol{R}^{T}\cdot\boldsymbol{\tau}\cdot\boldsymbol{R} = \tilde{\tau}^{ij}\tilde{\boldsymbol{g}}_{i}\otimes\tilde{\boldsymbol{g}}_{j}, \tag{34}$$

where $\tilde{\tau}^{ij}$ represent the contravariant components of the unrotated Kirchhoff stress tensor. Consequently, the Lie derivative of the Kirchhoff stress tensor leads to

$$L_{v}^{R}\left(\boldsymbol{\tau}\right) = \boldsymbol{R}_{*}\left[\frac{D}{Dt}\left\{\boldsymbol{R}^{*}\left(\boldsymbol{\tau}\right)\right\}\right] = \dot{\boldsymbol{\tau}} + \boldsymbol{\tau}\cdot\boldsymbol{\Omega} - \boldsymbol{\Omega}\cdot\boldsymbol{\tau} = \boldsymbol{\tau}^{\nabla G}, \tag{35}$$

where $\boldsymbol{\Omega}$ represents the rate of rotation tenor. The above equation is called the Green-McInnis-Naghdi stress rate of the Kirchhoff stress. It is noted that the unrotated Kirchhoff stress tensor may be represented in terms of the stored energy function as :

$$\tilde{\boldsymbol{\tau}} = 2\tilde{\rho}\frac{\partial\tilde{W}}{\partial\tilde{\boldsymbol{g}}}, \tag{36}$$

where $\tilde{\rho}$ represents the density in the unrotated configuration. Hence a new constitutive equation can be derived as

$${}_{R}L_{v}\left(\boldsymbol{\tau}\right) = 4\tilde{\rho}\frac{\partial^{2}\tilde{W}}{\partial\tilde{\boldsymbol{g}}\partial\tilde{\boldsymbol{g}}} : \boldsymbol{d}. \tag{37}$$

3. Constitutive Modeling for Hypo elasto-plastic Materials

The Cauchy's equation of motion can not be solved unless the relation between the first Piolar-Kirchhoff stress tensor and the acceleration or displacement is defined, because the first Piolar-Kirchhoff stress tensor depends on the deformation. Hence, that is why we need to introduce constitutive equations. Truesdell classified three elastic materials such as Cauchy elastic, hyperelastic, and hypoelastic materials. The Cauchy elastic material is one for which the Cauchy stress tensor can be written by a one-to-one mapping [12; 119]. It is noted that the current stress, the Cauchy stress, depends on only the current configuration, and not on the past history of the motion. Secondly, the hyperelastic, or Green-elastic, is one for which a strain energy function exists. Thirdly, a material is said to be hypoelastic, if any objective stress rate is a homogeneous linear function depending on the rate of deformation tensor and the Cauchy stress tensor as

$$\boldsymbol{\sigma}^{\nabla} = \bar{\mathfrak{M}}\left(\boldsymbol{\sigma}, \boldsymbol{d}\right), \tag{38}$$

where $\boldsymbol{\sigma}^{\nabla}$ denotes any objective rate of the Cauchy stress. The function $\bar{\mathfrak{M}}$ should be an objective function of the Cauchy stress tensor and the rate of deformation tensor. For most of hypoelastic materials, the function $\mathfrak{M}$ may be assumed to be linear between the objective Cauchy stress rate and the rate of deformation as seen below:

$$\boldsymbol{\sigma}^{\nabla} = \mathbb{C}\left(\boldsymbol{\sigma}\right) : \boldsymbol{d}, \tag{39}$$

where $\mathbb{C}\left(\boldsymbol{\sigma}\right)$ is the fourth-order tensor of elastic moduli depending on stress. Simo and Pister [11] proved that the use of the constant isotropic elasticity tensor of the infinitesimal in the hypoelasticity rate makes the material be inelastic due to the loss of the major symmetries of the elasticity tensors. Furthermore the hypoelasticity rate constitutive equations in which the elastic response of the rate of deformation tensor is characterized are also no longer appropriate for an elastic material due to the major symmetry failure. None the less, they concluded the assumption, particularly in the context of finite deformation metal plasticity, of the constant isotropic rate constitutive equation may be valid, **provided large volumetric strains do not occur**. In other word, the Jacobian should be almost one in the elastic region. It should be noted that the demonstrations given by Simo and Pister is contradictory to the arguments associated with the anomaly of the Jaumann stress rate as mentioned before. Hence in what follows, the hypoelastic rate constitutive equations we are about to investigate in phenomenological elastic-plastic materials with combined isotropic and kinematic hardening effects should be applied on the ground that the elastic strains are small compared to plastic strains and the large volumetric strains do not occur in the elastic deformation.

Table 1 Objective stress rates for hypoelastic rate constitutive equations

Stress Rates	Equations
Jaumann	$\boldsymbol{\sigma}^{\nabla J} = \dot{\boldsymbol{\sigma}} + \boldsymbol{\sigma}\cdot\boldsymbol{w} - \boldsymbol{w}\cdot\boldsymbol{\sigma}$
Jaumann	$\boldsymbol{\tau}^{\nabla J} = \dot{\boldsymbol{\tau}} + \boldsymbol{\tau}\cdot\boldsymbol{w} - \boldsymbol{w}\cdot\boldsymbol{\tau}$
Green-Naghdi	$\boldsymbol{\sigma}^{\nabla G} = \dot{\boldsymbol{\sigma}} + \boldsymbol{\sigma}\cdot\boldsymbol{\Omega} - \boldsymbol{\Omega}\cdot\boldsymbol{\sigma}$
Green-Naghdi	$\boldsymbol{\tau}^{\nabla G} = \dot{\boldsymbol{\tau}} + \boldsymbol{\tau}\cdot\boldsymbol{\Omega} - \boldsymbol{\Omega}\cdot\boldsymbol{\tau}$
Oldroyd	$\boldsymbol{\sigma}^{\nabla O} = \dot{\boldsymbol{\sigma}} - \boldsymbol{l}\cdot\boldsymbol{\sigma} - \boldsymbol{\sigma}\cdot\boldsymbol{l}^{T}$
Oldroyd	$\boldsymbol{\tau}^{\nabla O} = \dot{\boldsymbol{\tau}} - \boldsymbol{l}\cdot\boldsymbol{\tau} - \boldsymbol{\tau}\cdot\boldsymbol{l}^{T}$
Truesdell	$\boldsymbol{\sigma}^{\nabla T} = \dot{\boldsymbol{\sigma}} - \boldsymbol{l}\cdot\boldsymbol{\sigma} - \boldsymbol{\sigma}\cdot\boldsymbol{l}^{T} + \left(\boldsymbol{d} : \boldsymbol{I}\right)\boldsymbol{\sigma}$
Cotter-Rivlin	$\boldsymbol{\sigma}^{\nabla CR} = \dot{\boldsymbol{\sigma}} + \boldsymbol{l}^{T}\cdot\boldsymbol{\sigma} + \boldsymbol{\sigma}\cdot\boldsymbol{l}$
Cotter-Rivlin	$\boldsymbol{\tau}^{\nabla CR} = \dot{\boldsymbol{\tau}} + \boldsymbol{l}^{T}\cdot\boldsymbol{\tau} + \boldsymbol{\tau}\cdot\boldsymbol{l}$

It is generally assumed that the total velocity strain tensor $\boldsymbol{d}$ can be additively decomposed as follows:

$$\boldsymbol{d} = \boldsymbol{d}^{el} + \boldsymbol{d}^{pl}, \tag{40}$$

in which $\boldsymbol{d}^{el}$ and $\boldsymbol{d}^{pl}$ are the elastic and plastic parts respectively. In elastic-plastic analysis, the rate-independent constitutive equation of hypo elasto-plastic materials is defined as follows:

$$\boldsymbol{\sigma}^{\nabla} = \mathbb{C} : \boldsymbol{d}^{el}, \tag{41}$$

where $\boldsymbol{d}^{el}$ is of the total rate of deformation tensor. Notice that equation (41) is analogous to equation (39) in the sense of the form. We note that the total rate of deformation tensor is replaced by the elastic part of it. In other words, the elastic response of the material is hypoelastic. Therefore the elastic part of the total velocity strain tensor is linearly related to the material time rate of the Cauchy stress tensor. By the way, with the notion of hyperelasticity, we may have

$$\boldsymbol{\tau}^{\nabla} = \mathbb{C} : \boldsymbol{d}^{el}, \tag{42}$$

where is any objective stress rate of the Kirchhoff stress. In the sense of hyperelasticity, it can be observed that equation (42) implies that

$$\dot{\boldsymbol{S}} = \rho_0 \frac{\partial^2 \bar{W}(\boldsymbol{E})}{\partial \boldsymbol{E} \partial \boldsymbol{E}} : \dot{\boldsymbol{E}} \approx \frac{\partial^2 \hat{W}(\boldsymbol{E}^{el})}{\partial \boldsymbol{E}^{el} \partial \boldsymbol{E}^{el}} : \dot{\boldsymbol{E}}^{el}, \tag{43}$$

where $\boldsymbol{E}^{el}$ is the elastic part of the Green-strain tensor. It should be noted that $\boldsymbol{E}^{el}$ is different from the one of the intermediate configuration as shown in the literatures. In the spatial description, equation (43) may be rewritten:

$$L_v(\boldsymbol{\tau}) = \mathbb{C} : \boldsymbol{d}^{el}, \tag{44}$$

where $\mathbb{C}$ may be given by

$$\mathbb{C} = \lambda \boldsymbol{I} \otimes \boldsymbol{I} + 2\mu \boldsymbol{J}, \tag{45}$$

in which λ and μ are the Lamé coefficients and the identity tensors are given by

$$\boldsymbol{I} = \boldsymbol{g}_i \otimes \boldsymbol{g}^i, \ \boldsymbol{J} = \boldsymbol{g}_i \otimes \boldsymbol{g}_j \otimes \boldsymbol{g}^i \otimes \boldsymbol{g}^j. \tag{46}$$

Equation (44) becomes

$$L_v(\boldsymbol{\tau}) = \mathbb{C}^{ep}(\boldsymbol{\sigma}, \boldsymbol{d}) : \boldsymbol{d}. \tag{47}$$

It is noted that equation (47) retains a typical form of the rate constitutive equations for hypoelastic materials. It should importantly be realized that in the case of the elastic deformation, since equation (47) becomes the rate constitutive equation of the hypoelasticity of grade zero, the portion of elastic strains should be small compared with the one of plastic strains in order for equation (47) to be valid.

4. Determination of Jacobian

In this paper, the Kirchhoff and Cauchy formulations are referred to the formulation seen in [9]. In the Kirchhoff formulation, determination of the Jacobian is required to calculate the Kirchhoff stress tensor. The Jacobian indicates the determinant of the deformation gradient tensor, in which the deformation means a one-to-one mapping. A procedure to determine the Jacobian, which is required to calculate the Kirchhoff stress tensor, is presented. The following procedure is intended to apply for the Belytschko-Lin-Tsay shell element implementation [13].

The deformation gradient tensor is denoted as

$$\boldsymbol{F} = \frac{\partial \boldsymbol{x}}{\partial \boldsymbol{X}} = \frac{\partial (\boldsymbol{X} + \boldsymbol{u})}{\partial \boldsymbol{X}} = \boldsymbol{I} + \frac{\partial \boldsymbol{u}}{\partial \boldsymbol{X}}, \tag{48}$$

where is $\boldsymbol{u}$ the displacement vector. Introducing a corotational transformation matrix $\boldsymbol{Q}$, we have

$$\boldsymbol{F} = \boldsymbol{I} + \boldsymbol{Q} \cdot \frac{\partial \hat{\boldsymbol{u}}}{\partial \boldsymbol{X}}, \tag{49}$$

where $\hat{\boldsymbol{u}}$ is the displacement vector of a Belytschko-Lin-Tsay shell element in the corotational coordinates. The application of the chain rule to equation (49) results in

$$\boldsymbol{F} = \boldsymbol{I} + \boldsymbol{Q} \cdot \frac{\partial \hat{\boldsymbol{u}}}{\partial \hat{\boldsymbol{x}}} \cdot \frac{\partial \hat{\boldsymbol{x}}}{\partial \boldsymbol{X}} = \boldsymbol{I} + \boldsymbol{Q} \cdot \frac{\partial \hat{\boldsymbol{u}}}{\partial \hat{\boldsymbol{x}}} \cdot \boldsymbol{Q}^T, \tag{50}$$

where $\hat{\boldsymbol{x}}$ denotes the corotational coordinates in the Belytschko-Lin-Tsay shell element formulation. Since the Belytschko-Lin-Tsay shell element is based on the Mindlin theory of plates and shells, the displacement vector of a point in the shell may be expressed in terms of the translational displacement vector components $\left({}^m\hat{u}_x, {}^m\hat{u}_y, {}^m\hat{u}_z\right)$ and the rotational displacement vector components $\left(\hat{\phi}_x, \hat{\phi}_y, \hat{\phi}_z\right)$ of the midsurface by

$$\begin{Bmatrix} \hat{u}_x \\ \hat{u}_x \\ \hat{u}_x \end{Bmatrix} = \begin{Bmatrix} {}^m\hat{u}_x(\hat{x}, \hat{y}) + \hat{z}\ {}^m\hat{\phi}_y \\ {}^m\hat{u}_y(\hat{x}, \hat{y}) + \hat{z}\ {}^m\hat{\phi}_x \\ {}^m\hat{u}_z(\hat{x}, \hat{y}) \end{Bmatrix}. \tag{51}$$

In a bilinear quadrilateral element with single-point quadrature, we, hence, have the following expression

$$\frac{\partial \hat{\boldsymbol{u}}}{\partial \hat{\boldsymbol{x}}} = \begin{bmatrix} B_{1I}\ {}^m\hat{u}_{xI} & B_{2I}\ {}^m\hat{u}_{xI} & N_I\ {}^m\hat{\phi}_{yI} \\ B_{1I}\ {}^m\hat{u}_{yI} & B_{2I}\ {}^m\hat{u}_{yI} & N_I\ {}^m\hat{\phi}_{xI} \\ B_{1I}\ {}^m\hat{u}_{zI} & B_{2I}\ {}^m\hat{u}_{zI} & 0 \end{bmatrix}, \tag{52}$$

where Einstein's summation convention is applied over nodes, I = 1,…,4, and the shape function N_I may be written in terms of the isoparametric coordinates (ξ, η), as:

$$N_I = \frac{1}{4}(1 + \xi\xi_I)(1 + \eta\eta_I), \tag{53}$$

And the strain matrices B_{1I}, B_{2I} can be expressed as:

$$B_{1I} = \frac{\partial N_I}{\partial \hat{x}}, B_{2I} = \frac{\partial N_I}{\partial \hat{y}}. \tag{54}$$

Finally Jacobian can be determined by taking the determinant of the deformation gradient tensor

$$J = |\boldsymbol{F}|. \tag{55}$$

5. Numerical Examples

In this section, numerical examples are presented to serve the purpose of illustrating the accuracy and the effectiveness of the stress update procedures by the several objective stress rates derived so far. All the example results presented hereafter were obtained by a parallel transient dynamic code, GT-PARADYN [13], developed by the author, and in which the stress update algorithms proposed are inserted.

5.1 Spherical cap under pressure

As a non-contact example, a uniform pressure is imparted over the spherical cap as shown in the left-hand side of Fig. 1. The cap is clamped all round. Due to symmetry, only one quadrant of the cap is considered for the finite element model as shown in the left-hand side of Fig. 1. The material undergoes an elastic-plastic deformation with an isotropic hardening. Three integration points through the thickness are applied. The deflection curves for the center point by the several stress rates are compared in the right-hand side of Fig. 1. For

this case, any difference between results by the stress rates does not come out. The deflections of the center point are in good agreement with that by Belytschko [13] respectively.

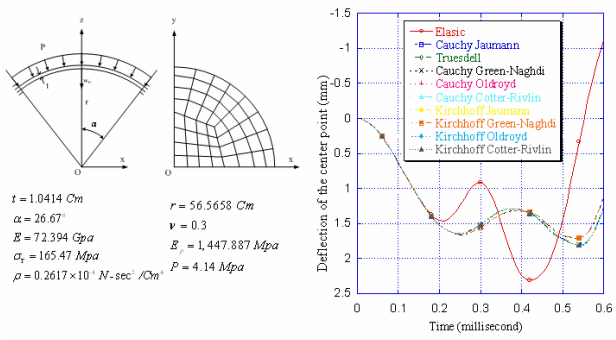

Fig. 1 Spherical cap center point displacement

5.2 Pipes impacting with both ends fixed

As a contact example, the two pipes are contacting toward each other, but circumferences of the lower pipe at both ends are clamped. All dimensions and properties are the same. Only the upper pipe is flying. For node 541 on the upper pipe, the deflection curves up to 160 milliseconds are compared in the right-hand side of Fig. 2. At about 80 milliseconds, the upper pipe seems to rebound. The graph indicates that the Kirchhoff stress formulation is more conservative and unstable than the Cauchy stress formulation.

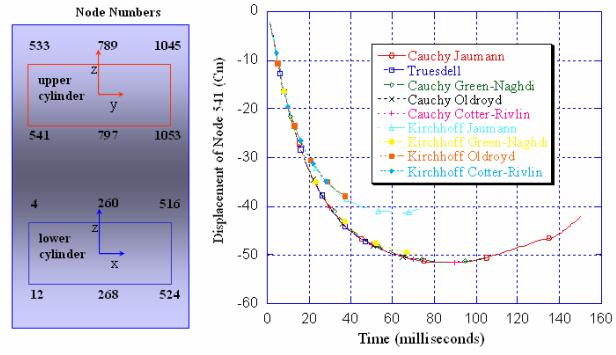

Fig. 2 Displacement of Node 541

6. Conclusions

Constitutive equations are established for hypo elasto-plastic materials. Several objective stress rates are derived by use of the Lie derivative. These stress rates are incorporated into the stress update algorithms proposed by the author. The algorithms are divided into two categories, including the Cauchy and Kirchhoff formulation. The difference among the stress rates are investigated for contact or non-contact examples. It is noted that the Kirchhoff stress formulation is more conservative for the contact problem. But, for non-contact examples, the same deflection curves are obtained. For the future work, the instability problem of the Kirchhoff stress formulation for the contact example will be solved along with a new contact algorithm.

Acknowledgements

Computations were performed on the IBM p690 at the Korea Institute of Science and Information Technology (KISTI). The support of KISTI is gratefully acknowledged.

References

(1) Truesdell, C., 1955, “Hypo-elsticity,” *J. Rat’l Mech. Anal.*, Vol. 4, pp. 83-133.
(2) Rivlin, R.S., 1955, “Further remarks on the stress-deformation relations for isotropic materials,” *J. Rat’l Mech. Anal.*, Vol. 4, pp. 681-702.
(3) McMeeking, R.M. and Rice, J.R., 1975, “Finite element formulations for problems of large elastic-plastic deformation,” *Int. J. Solids and Struct.*, Vol. 11, pp. 601-616.
(4) Dienes, J.K., 1979, “On the analysis of rotation and stress rate in deformation bodies,” *Acta Mechanica*, Vol. 32, pp. 217-232.
(5) Johnson, G.C. and Bammann, D.J., 1984, “A discussion of stress rates in finite deformation problem,” *Int. J. Solids Struct.*, Vol. 20, No. 8, pp. 725-737.
(6) Truesdell, C., 1953, “Corrections and additions to The mechanics foundations of elasticity and fluid dynamics,” *J. Rat’l Mech. Anal.*, Vol. 2, pp. 593-616.
(7) Oldroyd, J.G., 1950, “On the formulation of rheological equations of state,” *Proc. Roy. Soc. London*, A200, pp. 523-541.
(8) Cotter, B.A. and Rivlin, R.S., 1955, “Tensors associated with time-dependent stress,” *Quarterly Appl. Math.*, Vol. 13, pp. 177-182.
(9) Har, J., 2003, “On application of radial return method to transient shell dynamics,” Proc. Solid and Struct. Mech. Div. KSME 2003.
(10) Doyle, T.C. and Ericksen, J.L., 1956, “Nonlinear elasticity,” in: Advances in Applied Mechanics IV, Academic Press, New York.
(11) Simo, J.C. and Pister, K.S., 1984, “Remarks on rate constitutive equations for finite deformation problems: computational implications,” *Comp. Meth. Appl. Mech. Engrg.*, Vol. 46, pp. 201-215.
(12) Truesdell, C. and Noll, W., 1992, The non-linear field theories of mechanics, 2nd ed., Springer-Verlag, Berlin.
(13) Har, J. and Fulton, R.E., 2003, “A parallel finite element procedure for contact-impact problems,” *Engineering with Computers*, Vol. 19, pp. 67-84.